HHS Public Access

Author manuscript

Endocrine. Author manuscript; available in PMC 2020 September 01.

Published in final edited form as:

Endocrine. 2018 August ; 61(2): 216–223. doi:10.1007/s12020-018-1617-1.

Molecular evaluation of a sporadic paraganglioma with concurrent *IDH1* and *ATRX* mutations

Jing Zhang[#1,2], **Jingjing Jiang**[#1,2], **Yu Luo**[1], **Xiaomu Li**[1], **Zhiqiang Lu**[1], **Yujun Liu**[3], **Jie Huang**[4], **Yingyong Hou**[4], **Ying Pang**[5], **Mitchell Yee Fong Sun**[6], **Tracy S. Wang**[7], **Douglas B. Evans**[7], **Karel Pacak**[5], **Zhengping Zhuang**[8], **Xin Gao**[1,2]

[1]Department of Endocrinology and Metabolism, Zhongshan Hospital, Fudan University, Shanghai, China

[2]Fudan Institute for Metabolic Diseases, Fudan University, Shanghai, China

[3]Department of Urology, Zhongshan Hospital, Fudan University, Shanghai, China

[4]Department of Pathology, Zhongshan Hospital, Fudan University, Shanghai, China

[5]Section on Medical Neuroendocrinology, Eunice Kennedy Shriver National Institute of Child Health and Human Development, Bethesda, MD, USA

[6]College of Liberal Arts and Sciences, University of Illinois at Chicago, Chicago, IL, USA

[7]Department of Surgery, Medical College of Wisconsin, Milwaukee, WI, USA

[8]Surgical Neurology Branch, National Institute of Neurological Disorders and Stroke, National Institutes of Health, Bethesda, MD, USA

[#] These authors contributed equally to this work.

Abstract

Purpose—Pheochromocytomas and paragangliomas (PPGLs) are neuroendocrine tumors of neural crest origin. Germline or somatic mutations of numerous genes have been implicated in the pathogenesis of PPGLs, including the isocitrate dehydrogenase 1 (*IDH1*) gene and alpha thalassemia/mental retardation syndrome X-linked (*ATRX*) gene. Although concurrent *IDH1* and *ATRX* mutations are frequently seen in gliomas, they have never been reported together in PPGLs. The aim of this study was to characterize one paraganglioma with concurrent *IDH1* and *ATRX* mutations identified by whole exome sequencing.

Xin Gao gao.xin@zs-hospital.sh.cn happy20061208@126.com.

Compliance with ethical standards

Ethical approval All the procedures performed in studies involving human participants were in accordance with the ethical standards of the institutional and national research committee and with the 1964 Helsinki declaration, and its later amendments or comparable ethical standards. The study was approved by the institutional review board of Zhongshan Hospital, Fudan University.

Informed consent Informed consent was obtained from all individual participants included in the study.

Electronic supplementary material The online version of this article (https://doi.org/10.1007/s12020-018-1617-1) contains supplementary material, which is available to authorized users.

Conflict of interest The authors declare that they have no conflict of interest.

Methods—Leukocyte and tumor DNA were used for whole exome sequencing and Sanger sequencing. 2-hydroxyglurarate level and the global DNA methylation status in the tumor were measured. ATRX's cDNA transcripts were analyzed. Tyrosine hydroxylase (TH), HIF1α and ATRX staining, as well as telomere-specific FISH was also performed.

Results—The presence of a somatic *IDH1* (c.394C>T, p.R132C) mutation and a concurrent somatic *ATRX* splicing mutation (c.4318–2A>G) in the current case was confirmed. Dramatic accumulation of 2-hydroxyglutarate was detected in the paraganglioma without the global DNA hypermethylation, and pseudohypoxia was also activated. Importantly, immunohistochemistry revealed negative TH staining in the tumor and the first exon region of *TH* gene was hypermethylated resulting in normal plasma metanephrines. The splicing *ATRX* mutation resulted in two transcripts, causing frameshifts. Immunohistochemistry revealed scarce ATRX staining in the tumor. Alternative lengthening of telomeres (ALT) was detected by FISH.

Conclusions—This case represents the first concurrence of *IDH1* and *ATRX* mutations in PPGLs. Although relatively rare, a somatic R132C mutation of *IDH1* might play a role in a small subset of sporadic PPGLs.

Keywords

Paraganglioma; *IDH1*; *ATRX*; Somatic mutations

Introduction

Pheochromocytomas and paragangliomas (PPGLs) are neuroendocrine tumors of neural crest origin. PPGLs carry the highest degree of heritability among all the tumors, with at least one-third of PPGL patients possessing disease-causing germline mutations [1]. Germline or somatic mutations of an increasing number of genes have been implicated in the pathogenesis of PPGLs, including the *IDH1* gene and *ATRX* gene. IDH1 is a key enzyme in the Krebs cycle that normally decarboxylates isocitrate to α-ketoglutarate (α-KG) with accompanying reduction of NADP to NADPH. Somatic *IDH1* mutation at R132 has been previously reported in gliomas and acute myeloid leukemia (AML) [2, 3]. The mutation alters the function of the enzyme by favoring reverse conversion of NADPH to NADP and metabolism of α-ketoglutarate to the D isomer of 2-hydroxyglutarate (2-HG), an oncometabolite [4, 5]. 2-hydroxyglutarate competitively inhibits α-KG-dependent dioxygenases, leading to global histone and DNA hypermethylation [6]. However, the *IDH1* mutation is extremely rare in PPGLs and remains to be confirmed by more cases [7, 8].

ATRX is a large gene located on the X chromosome, whose protein plays an important role in telomere maintenance and chromosome integrity [9]. Somatic *ATRX* mutations have been reported in glioma [10], pancreatic neuroendocrine tumors [11], pediatric osteosarcoma [12], and recently in PPGLs [13]. Tumors with inactivating *ATRX* mutations frequently associates with alternative lengthening of telomeres (ALT), and the ALT phenotype is observed in 5%–15% of human cancers [14].

IDH1 mutations are frequently accompanied by *ATRX*-inactivating mutations in adult gliomas, especially astrocytomas [15], but this association has not been reported in other

tumors so far. Here, we report a heterozygous *IDH1* mutation accompanied by *ATRX* mutation in one paraganglioma, identified by whole-exome sequencing.

Materials and methods

Whole-exome sequencing and analysis

Tumor DNA was extracted using a phenol-chloroform method, and blood DNA was extracted using a commercial blood DNA extraction kit (Tiangen, China). Tumor DNA and the matched blood DNA samples were used for whole-exome sequencing. Library preparation and exome enrichment were prepared using Illumina TruSeq Sample Prep kits and Agilent SureSelect Human All Exon v5 kit. Briefly, 1–2 μg of DNA was randomly fragmented by Covaris. Fragments were end repaired, and an extra A base was added to the 3′ end. DNA was quantified by Agilent 2100 Bioananlyzer and concentration was measured using a Qubit. Each captured library was sequenced on the Illumina HiSeq 4000. The resulting fastq data were aligned to the human reference genome (hg19) using the Burrows-Wheeler Aligner (BWA).

Sanger sequencing

Mutations detected by whole-exome sequencing were validated by direct Sanger sequencing using the same DNA samples. Primers were designed across the mutation sites (Table S3). Polymerase chain reaction (PCR) conditions were as follows: preheating at 95 °C for 5 min, 30 cycles of 95 °C for 30 sec, 62 °C for 30 sec, and 72 °C for 45 sec, followed by 72 °C for 10 min. PCR products were sequenced with BigDye Terminator v3.1 sequencing kit and then analyzed on the ABI Prism 3730xl Genetic Analyzer. Mutation Surveyor V4.0.8 was used to analyze the sequence traces.

Metabolite extraction and gas chromatography-mass spectrometer (GC-MS) analysis

Metabolites in the tumors with or without *IDH1* mutation (70 mg of tumor from each patient) were extracted and GC-MS analysis were performed, as previously described [16].

DNA methylation array

Whole-genome DNA methylation was analyzed in the *IDH1*-mutant paraganglioma and the normal adrenal medulla samples using Illumina HumanMethylationEPIC array, as previously described [17]. The raw data were used to calculate the beta value DNA methylation scores for each probe and sample.

PCR-based Sanger sequencing of ATRX's cDNA and real-time PCR

Total RNA was extracted from tumor tissues with the TRIzol reagent (Invitrogen, Carlsbad, CA, USA), according to the manufacturer's protocol. Total RNA (1ug) was used to synthesize the first-strand cDNA with the PrimeScript™ RT reagent Kit (TaKaRa Bio, Japan). Forward primers on exon 13 and exon 14 and reverse primers on exon 16 and exon 17 were designed to amplify the different transcriptions of *ATRX* (Table S3). The PCR products of each primer pair were sequenced using an ABI 3730xl DNA Analyzer (Applied Biosystems, Foster City, CA, USA). The joint points of different regions were identified by

CodonCode Aligner (CodonCode Corporation, Centerville, MA, USA) or deduced manually after aligning to the reference sequence.

Levels of mRNA expression of *TH*, *VEGFA*, *PGK1*, *GNA14*, *PCSK6*, *EDN1*, and *ACTB* were examined by real-time quantitative PCR on the Roche LightCycler 480 system using KOD SYBR qPCR Mix (TOYOBO, Japan) and primers (Table S3). PCR conditions were as follows: one cycle of 98 °C for 2 min, 45 cycles of 98 °C for 10 s, 60 °C for 10 s, and 68 °C for 30 s. The data were analyzed using the comparative threshold cycle method.

Bisulfite genomic sequencing analysis

Genomic DNA was isolated using E.Z.N.A. Tissue DNA Kit (Omega, USA), and bisulfite modification of genomic DNA was performed using EZ DNA Methylation-Gold Kit (Zymo Research, USA), according to the manufacturer's protocol. Genomic DNA, bisulfite-modified genomic DNA (50 ng), and primers (Table S3) were used in a PCR reaction to amplify the first exon region of the *TH* gene. PCR products were sequenced by Sanger sequencing, as described above.

Immunohistochemistry

The paraffin-embedded tumors were incised into 5-μm thick slices. Slides were de-paraffinized by incubating in xylene and rehydrating in graded ethanol. Antigens were retrieved by incubating in citrate buffer at 95 °C for 20 min. Specimens were then incubated with 3% H_2O_2 and blocked with a blocking buffer (Sigma-Aldrich, USA). The slides were probed with anti-HIF1α antibody(1:400, Sigma, USA), anti-TH antibody (1:200, Abcam, USA), or anti-ATRX antibody (1:1000, Sigma, USA) overnight at 4 °C and developed by DAB substrate.

Telomere-specific fluorescence in situ hybridization (FISH)

Telomere-specific FISH was performed, as previously described [10]. Images were taken using Olympus DP73 fluorescent microscope imaging system.

Results

Clinical characteristics

The patient was a 69-year-old man presenting with dizziness, constipation, and hypertension for a month. Single photon emission computed tomography/computed tomography (SPECT/CT) identified a right retroperitoneal mass (5.8 × 4.2 cm) positive on the somatostatin receptor and scintigraphy labeled with Technetium-99m-octreotide (Fig. 1a). Plasma metanephrine level (74.4 pg/ml, reference range <96.6 pg/ml) and normetanephrine level (56 pg/ml, reference range <163 pg/ml) were within normal, while plasma chromogranin A level was elevated (441.3 ng/ml, reference range: 27–94 ng/ml) and catecholamines levels within the tumor were very low (Table S1, S2). The patient had no previous history of glioma, acute myeloid leukemia, or chondrosarcoma. Following removal, the mass's gross appearance and histopathology were consistent with a paraganglioma.

Concurrent somatic *IDH1* and *ATRX* mutations were identified

Whole-exome sequencing identified two heterozygous mutations in the tumor: an *IDH1* mutation (c.394C > T, p. R132C) and an *ATRX* mutation (c.4318–2A > G), confirmed by Sanger sequencing (Fig. 1b). The mutations were not identified in the matched-blood DNA by direct sequencing, implying its somatic nature (Fig. 1b). Other somatic or germline mutations in the known PPGL pathogenic genes were not identified in the paraganglioma.

Accumulation of 2-hydroxyglutarate was detected in the tumor without the global DNA hypermethylation

To determine whether the somatic *IDH1* (R132C) mutation was functioning in the current paraganglioma, metabolites from freshly frozen tumors with or without *IDH1* (R132C) mutation were analyzed by GC-MS. As expected, dramatic accumulation of 2-hydroxyglutarate was detected in the *IDH1* (R132C) mutant tumor, whereas 2-hydroxyglutarate was almost undetectable in the control tumors without *IDH1* mutation (Fig. 1c). To our surprise, in the current paraganglioma, despite significant accumulation of 2-hydroxyglutarate, the global methylation status was similar to that of a normal adrenal medulla control based beta value, calculated from Illumina HumanMethylationEPIC array (Fig. 1d).

Almost no expression of tyrosine hydroxylase (TH) and hypermethylation in the first exon region of the *TH* gene

Immunohistochemistry revealed scarce TH staining in the tumor (Fig. 2d). The mRNA level of the *TH* gene encoding TH was almost undetectable, compared with that of a normal adrenal medulla (Fig. 1e), which consisted with subsequently low tumor tissue concentrations of catecholamines and normal plasma concentrations of metanephrines (Table S1, S2). A previous study has related the expression of the *TH* gene to the methylation level in the first exon region [18], unfortunately, this area was not covered by the Illumina HumanMethylationEPIC array. We performed methylation-specific PCR and confirmed that this region was indeed hypermethylated in the tumor, compared with normal adrenal medulla or catecholamine-secreting PPGLs (Fig. 1g).

HIF1α staining was positive, and hypoxia-related genes were upregulated

Hypoxia inducible factor 1 alpha (HIF1α) staining was strongly positive in the *IDH1*-mutant tumor (Fig. 2e). Consistently, multiple HIF target genes including *EDN1*, *VEGFA*, *PGK1*, *GNA14*, and *PCSK6* were upregulated in the tumor, compared with normal adrenal medulla (Fig. 1e), suggesting that pseudohypoxia was activated in the *IDH1*-mutant tumor.

Splicing mutation of *ATRX* resulted in alternative transcripts, scarce ATRX staining and ALT

In the current case, the somatic-splicing mutation (c.4318–2A > G) of *ATRX* gene was predicted to affect exon 15 because it occurred 2 base pairs away from the 5′ end. One transcript skipped the first 2 base pairs of the exon 15, while the other one skipped the entire exon 15 (Fig. 1h). Both transcripts resulted in frameshifts and the predicted protein products lost more than 1000 amino acids in the C-terminal, which encompassed an important

functional helicase domain. ATRX staining was sparse in the current tumor, with most cells losing the ATRX staining in the nucleus (Fig. 2c). As expected, ALT was detected by telomere-specific FISH (Fig. 1f).

Discussion

Here, we report a somatic heterozygous *IDH1* (c.394C > T, p.R132C) mutation accompanied by somatic *ATRX* (c.4318–2A > G)-splicing mutation in one paraganglioma patient. In gliomas, *IDH1* mutations are very-early genetic events in a common glial precursor cell population with a well-established pathogenic role [19]. Consistent with previous studies, the heterozygous R132C mutant paraganglioma in our study had an extremely high level of 2-hydroxyglutarate—direct evidence that the mutant IDH1 enzyme was active. High level of 2-hydroxyglutarat may inhibit an important demethylation enzyme Ten-eleven translocase-2 (TET2), leading to a global CpG island methylator phenotype and gene silencing [5, 20]. Surprisingly, our paraganglioma showed the absence of the hypermethylator phenotype, though the methylation status mighthave been complicated by *ATRX* mutation as well.

IDH1 mutations are extremely rare in PPGLs, to our knowledge, three paragangliomas with somatic *IDH1* mutations have been documented in literature [1, 7, 21]. The three previous cases and our current case together reveal some interesting common features: 1. They all had extra-adrenal paragangliomas; 2. They were old and the clinical behaviors of the tumors appeared benign at diagnosis; and 3. All tumors carried the relatively rare R132C somatic mutation, instead of the most common R132H mutation (Table S4). In patients with gliomas and AMLs, *IDH1* mutations were generally associated with favorable prognosis; a recent study revealed that accumulation of the oncometabolite 2-hydroxyglutarate exhibits anti-proliferation effects, while it contributes to cancer initiation [22]. Likewise, these *IDH1*-mutant paragangliomas exhibited no sign of malignancy at diagnosis, though long-term follow-up is needed, since metastasis can occur more than 20 years later.

Recent studies have classified PPGLs mutations into three main clusters based on their gene expression profiles: pseudohypoxia group, Wnt-signaling group, and kinase-signaling group [1, 23]. Cluster-one tumors are characterized by constitutive activation of the hypoxia-angiogenesis pathways, regardless of the oxygen levels (pseudohypoxia) [24]. Mutations of key enzymes of the Krebs cycle usually cause a pseudohypoxia effect [23]. Pseudohypoxia was activated in the *IDH1*-mutant tumor, confirming *IDH1* as a cluster-one gene.

It should be noted that plasma metanephrines were normal in the current case and catecholamines levels within the tumor were much lower than that of normal adrenal medulla. Furthermore, TH staining was negative and the mRNA level of the *TH* gene was almost undetectable, suggesting that the tumor was incapable of synthesizing excessive catecholamines. The hypermethylation of the *TH* gene in the *IDH1*-mutant paraganglioma was intriguing, previous studies have found that reduced *TH* gene expression correlated with DNA methylation of *TH* gene itself in various cell lines, rat adrenal medulla, and human brain tissues [18, 25]. Given the profound effect of *IDH1* on methylation, it would be interesting to investigate whether *TH* promoter methylation was directly affected by the

IDH1 mutation. This might also explain a small subset of catechomaline-negative PPGLs derived from sympathetic paravertebral ganglia.

Somatic mutations in the *ATRX* gene have recently been related to PPGLs, with varied prevalence [13, 26]; *ATRX* splicing mutations are rare and usually destabilize the RNA transcripts, resulting in scarce expression of ATRX protein. Consistently, ATRX staining was sparse in the current tumor, with the majority of cells losing the ATRX staining in the nucleus. The ATRX complex functions in the heterochromatin assembly at telomeres, whose shortening is related to senescence and aging [27]. While most tumors rely on telomerase to maintain long telomeres and achieve immortalization, approximately 10–15% of non-epithelial tumors (such as gliomas) utilize a telomerase-independent mechanism: ALT—commonly associated with high levels of telomeric instability [28]. Astrocytomas and pancreatic neuroendocrine tumors with inactivating *ATRX* mutations frequently display evidence of ALT [28]. Less often, ALT has been reported in some of PPGLs carrying *ATRX* mutations. In the current case, ALT was detected by telomere-specific FISH. Notably, *ATRX* mutations alone do not trigger ALT [29]; the relationship between *ATRX* mutation and ALT in PPGLs remains to be further investigated by additional cases.

Concurrent somatic *IDH1* and *ATRX* mutations are very common in gliomas, particularly in the astrocytoma subtype [15]. In contrast, concurrent germline or somatic mutations in more than one pathogenic gene in PPGLs are rare [1]. However, somatic *ATRX* mutation is an exception and is frequently associated with hereditary *SDHB* mutations in PPGLs [1, 13]. In the current paraganglioma, somatic *IDH1* mutation, instead of germline *SDHB* mutation, was found to coexist with somatic *ATRX* mutation—resembling a common cooperation between *ATRX* and *IDH1* mutations in gliomas. The collaboration between *IDH1* and *ATRX* mutations in tumors is not well understood. A generation of mouse models lacking ATRX expression in conjunction with *IDH1* R132 mutations in specific cell types would be an excellent way to decipher the underlying molecular events in future.

In summary, our case indicates that the rare somatic R132C mutation of *IDH1* might play a role in a small subset of sporadic PPGLs and—just like in gliomas—*IDH1* and *ATRX* mutations can coexist in PPGLs.

Supplementary Material

Refer to Web version on PubMed Central for supplementary material.

Acknowledgements

We thank Dr. Dan Ye from Institute of Biomedical Sciences Fudan University and Dr. Jingmin Yang from Shanghai WeHealth BioMedical Technology Co., Ltd for the technical assistance.

Funding This study was funded by the National Natural Science Foundation of China (Grant number: 81471016) and, in part, by the Intramural Research Program of the NIHNCI, NINDS, and Eunice Kennedy Shriver NICHD.

References

1. Fishbein L, Leshchiner I, Walter V, Danilova L, Robertson AG, Johnson AR, Lichtenberg TM, Murray BA, Ghayee HK, Else T, Ling S, Jefferys SR, de Cubas AA, Wenz B, Korpershoek E,

Amelio AL, Makowski L, Rathmell WK, Gimenez-Roqueplo AP, Giordano TJ, Asa SL, Tischler AS; Cancer N. Genome Atlas Research, Pacak K, Nathanson KL, Wilkerson MD, Comprehensive molecular characterization of pheochromocytoma and paraganglioma. Cancer Cell 31, 181–193 (2017) [PubMed: 28162975]

2. Parsons DW, Jones S, Zhang X, Lin JC, Leary RJ, Angenendt P, Mankoo P, Carter H, Siu IM, Gallia GL, Olivi A, McLendon R, Rasheed BA, Keir S, Nikolskaya T, Nikolsky Y, Busam DA, Tekleab H, Diaz LA Jr., Hartigan J, Smith DR, Strausberg RL, Marie SK, Shinjo SM, Yan H, Riggins GJ, Bigner DD, Karchin R, Papadopoulos N, Parmigiani G, Vogelstein B, Velculescu VE, Kinzler KW, An integrated genomic analysis of human glioblastoma multiforme. Science 321, 1807–1812 (2008) [PubMed: 18772396]
3. Mardis ER, Ding L, Dooling DJ, Larson DE, McLellan MD, Chen K, Koboldt DC, Fulton RS, Delehaunty KD, McGrath SD, Fulton LA, Locke DP, Magrini VJ, Abbott RM, Vickery TL, Reed JS, Robinson JS, Wylie T, Smith SM, Carmichael L, Eldred JM, Harris CC, Walker J, Peck JB, Du F, Dukes AF, Sanderson GE, Brummett AM, Clark E, McMichael JF, Meyer RJ, Schindler JK, Pohl CS, Wallis JW, Shi X, Lin L, Schmidt H, Tang Y, Haipek C, Wiechert ME, Ivy JV, Kalicki J, Elliott G, Ries RE, Payton JE, Westervelt P, Tomasson MH, Watson MA, Baty J, Heath S, Shannon WD, Nagarajan R, Link DC, Walter MJ, Graubert TA, DiPersio JF, Wilson RK, Ley TJ, Recurring mutations found by sequencing an acute myeloid leukemia genome. N. Engl. J. Med 361, 1058–1066 (2009) [PubMed: 19657110]
4. Dang L, White DW, Gross S, Bennett BD, Bittinger MA, Driggers EM, Fantin VR, Jang HG, Jin S, Keenan MC, Marks KM, Prins RM, Ward PS, Yen KE, Liau LM, Rabinowitz JD, Cantley LC, Thompson CB, Vander Heiden MG, Su SM, Cancer-associated IDH1 mutations produce 2-hydroxyglutarate. Nature 462, 739–744 (2009) [PubMed: 19935646]
5. Figueroa ME, Abdel-Wahab O, Lu C, Ward PS, Patel J, Shih A, Li Y, Bhagwat N, Vasanthakumar A, Fernandez HF, Tallman MS, Sun Z, Wolniak K, Peeters JK, Liu W, Choe SE, Fantin VR, Paietta E, Lowenberg B, Licht JD, Godley LA, Delwel R, Valk PJ, Thompson CB, Levine RL, Melnick A, Leukemic IDH1 and IDH2 mutations result in a hypermethylation phenotype, disrupt TET2 function, and impair hematopoietic differentiation. Cancer Cell 18, 553–567 (2010) [PubMed: 21130701]
6. Xu W, Yang H, Liu Y, Yang Y, Wang P, Kim SH, Ito S, Yang C, Wang P, Xiao MT, Liu LX, Jiang WQ, Liu J, Zhang JY, Wang B, Frye S, Zhang Y, Xu YH, Lei QY, Guan KL, Zhao SM, Xiong Y, Oncometabolite 2-hydroxyglutarate is a competitive inhibitor of alpha-ketoglutarate-dependent dioxygenases. Cancer Cell 19, 17–30 (2011) [PubMed: 21251613]
7. Gaal J, Burnichon N, Korpershoek E, Roncelin I, Bertherat J, Plouin PF, de Krijger RR, Gimenez-Roqueplo AP, Dinjens WN, Isocitrate dehydrogenase mutations are rare in pheochromocytomas and paragangliomas. J. Clin. Endocrinol. Metab 95, 1274–1278 (2010) [PubMed: 19915015]
8. Yao L, Barontini M, Niederle B, Jech M, Pfragner R, Dahia PL, Mutations of the metabolic genes IDH1, IDH2, and SDHAF2 are not major determinants of the pseudohypoxic phenotype of sporadic pheochromocytomas and paragangliomas. J. Clin. Endocrinol. Metab 95, 1469–1472 (2010) [PubMed: 20130071]
9. Watson LA, Goldberg H, Berube NG, Emerging roles of ATRX in cancer. Epigenomics 7, 1365–1378 (2015) [PubMed: 26646632]
10. Heaphy CM, de Wilde RF, Jiao Y, Klein AP, Edil BH, Shi C, Bettegowda C, Rodriguez FJ, Eberhart CG, Hebbar S, Offerhaus GJ, McLendon R, Rasheed BA, He Y, Yan H, Bigner DD, Oba-Shinjo SM, Marie SK, Riggins GJ, Kinzler KW, Vogelstein B, Hruban RH, Maitra A, Papadopoulos N, Meeker AK, Altered telomeres in tumors with ATRX and DAXX mutations. Science 333, 425 (2011) [PubMed: 21719641]
11. Jiao Y, Shi C, Edil BH, de Wilde RF, Klimstra DS, Maitra A, Schulick RD, Tang LH, Wolfgang CL, Choti MA, Velculescu VE, Diaz LA Jr., Vogelstein B, Kinzler KW, Hruban RHN, Papadopoulos, DAXX/ATRX, MEN1, and mTOR pathway genes are frequently altered in pancreatic neuroendocrine tumors. Science 331, 1199–1203 (2011) [PubMed: 21252315]
12. Chen X, Bahrami A, Pappo A, Easton J, Dalton J, Hedlund E, Ellison D, Shurtleff S, Wu G, Wei L, Parker M, Rusch M, Nagahawatte P, Wu J, Mao S, Boggs K, Mulder H, Yergeau D, Lu C, Ding L, Edmonson M, Qu C, Wang J, Li Y, Navid F, Daw NC, Mardis ER, Wilson RK, Downing JR, Zhang J, Dyer MA; St. Jude Children's Research Hospital-Washington University Pediatric

Cancer Genome, P., Recurrent somatic structural variations contribute to tumorigenesis in pediatric osteosarcoma. Cell Rep. 7, 104–112 (2014) [PubMed: 24703847]

13. Fishbein L, Khare S, Wubbenhorst B, DeSloover D, D'Andrea K, Merrill S, Cho NW, Greenberg RA, Else T, Montone K, LiVolsi V, Fraker D, Daber R, Cohen DL, Nathanson KL, Whole-exome sequencing identifies somatic ATRX mutations in pheochromocytomas and paragangliomas. Nat. Commun 6, 6140 (2015) [PubMed: 25608029]
14. Heaphy CM, Subhawong AP, Hong SM, Goggins MG, Montgomery EA, Gabrielson E, Netto GJ, Epstein JI, Lotan TL, Westra WH, Shih Ie M, Iacobuzio-Donahue CA, Maitra A, Li QK, Eberhart CG, Taube JM, Rakheja D, Kurman RJ, Wu TC, Roden RB, Argani P, De Marzo AM, Terracciano L, Torbenson M, Meeker AK, Prevalence of the alternative lengthening of telomeres telomere maintenance mechanism in human cancer subtypes. Am. J. Pathol 179, 1608–1615 (2011) [PubMed: 21888887]
15. Cancer N. Genome Atlas Research, Brat DJ, Verhaak RG, Aldape KD, Yung WK, Salama SR et al. Comprehensive, integrative genomic analysis of diffuse lower-grade gliomas. N. Engl. J. Med 372, 2481–2498 (2015) [PubMed: 26061751]
16. Ma S, Jiang B, Deng W, Gu ZK, Wu FZ, Li T, Xia Y, Yang H, Ye D, Xiong Y, Guan KL, D-2-hydroxyglutarate is essential for maintaining oncogenic property of mutant IDH-containing cancer cells but dispensable for cell growth. Oncotarget 6, 8606–8620 (2015) [PubMed: 25825982]
17. Moran S, Arribas C, Esteller M, Validation of a DNA methylation microarray for 850,000 CpG sites of the human genome enriched in enhancer sequences. Epigenomics 8, 389–399 (2016) [PubMed: 26673039]
18. Aranyi T, Faucheux BA, Khalfallah O, Vodjdani G, Biguet NF, Mallet J, Meloni R, The tissue-specific methylation of the human tyrosine hydroxylase gene reveals new regulatory elements in the first exon. J. Neurochem 94, 129–139 (2005) [PubMed: 15953356]
19. Watanabe T, Nobusawa S, Kleihues P, Ohgaki H, IDH1 mutations are early events in the development of astrocytomas and oligodendrogliomas. Am. J. Pathol 174, 1149–1153 (2009) [PubMed: 19246647]
20. Noushmehr H, Weisenberger DJ, Diefes K, Phillips HS, Pujara K, Berman BP, Pan F, Pelloski CE, Sulman EP, Bhat KP, Verhaak RG, Hoadley KA, Hayes DN, Perou CM, Schmidt HK, Ding L, Wilson RK, Van Den Berg D, Shen H, Bengtsson H, Neuvial P, Cope LM, Buckley J, Herman JG, Baylin SB, Laird PW, Aldape K; Cancer N. Genome Atlas Research, Identification of a CpG island methylator phenotype that defines a distinct subgroup of glioma. Cancer Cell. 17, 510–522 (2010) [PubMed: 20399149]
21. Remacha L, Comino-Mendez I, Richter S, Contreras L, Curras-Freixes M, Pita G, Leton R, Galarreta A, Torres-Perez R, Honrado E, Jimenez S, Maestre L, Moran S, Esteller M, Satrustegui J, Eisenhofer G, Robledo M, Cascon A, Targeted exome sequencing of krebs cycle genes reveals candidate cancer-predisposing mutations in pheochromocytomas and paragangliomas. Clin. Cancer Res 23, 6315–6324 (2017) [PubMed: 28720665]
22. Su R, Dong L, Li C, Nachtergaele S, Wunderlich M, Qing Y, Deng X, Wang Y, Weng X, Hu C, Yu M, Skibbe J, Dai Q, Zou D, Wu T, Yu K, Weng H, Huang H, Ferchen K, Qin X, Zhang B, Qi J, Sasaki AT, Plas DR, Bradner JE, Wei M, Marcucci G, Jiang X, Mulloy JC, Jin J, He C, Chen J, R-2HG exhibits anti-tumor activity by targeting FTO/m(6)A/MYC/CEBPA Signaling. Cell 172, 90–105 e123 (2018)
23. Crona J, Taieb D, Pacak K, New perspectives on pheochromocytoma and paraganglioma: toward a molecular classification. Endocr. Rev 38, 489–515 (2017) [PubMed: 28938417]
24. Gruber M, Simon MC, Hypoxia-inducible factors, hypoxia, and tumor angiogenesis. Curr. Opin. Hematol 13, 169–174 (2006) [PubMed: 16567961]
25. Okuse K, Matsuoka I, Kurihara K, Tissue-specific methylation occurs in the essential promoter element of the tyrosine hydroxylase gene. Mol. Brain Res 46, 197–207 (1997) [PubMed: 9191094]
26. Toledo RA, Qin Y, Cheng ZM, Gao Q, Iwata S, Silva GM, Prasad ML, Ocal IT, Rao S, Aronin N, Barontini M, Bruder J, Reddick RL, Chen Y, Aguiar RC, Dahia PL, Recurrent mutations of chromatin-remodeling genes and kinase receptors in pheochromocytomas and paragangliomas. Clin. Cancer Res 22, 2301–2310 (2016) [PubMed: 26700204]
27. Harley CB, Futcher AB, Greider CW, Telomeres shorten during ageing of human fibroblasts. Nature 345, 458–460 (1990) [PubMed: 2342578]

28. Cesare AJ, Reddel RR, Alternative lengthening of telomeres: models, mechanisms and implications. Nat. Rev. Genet 11, 319–330 (2010) [PubMed: 20351727]

29. Flynn RL, Cox KE, Jeitany M, Wakimoto H, Bryll AR, Ganem NJ, Bersani F, Pineda JR, Suva ML, Benes CH, Haber DA, Boussin FD, Zou L, Alternative lengthening of telomeres renders cancer cells hypersensitive to ATR inhibitors. Science 347, 273–277 (2015) [PubMed: 25593184]

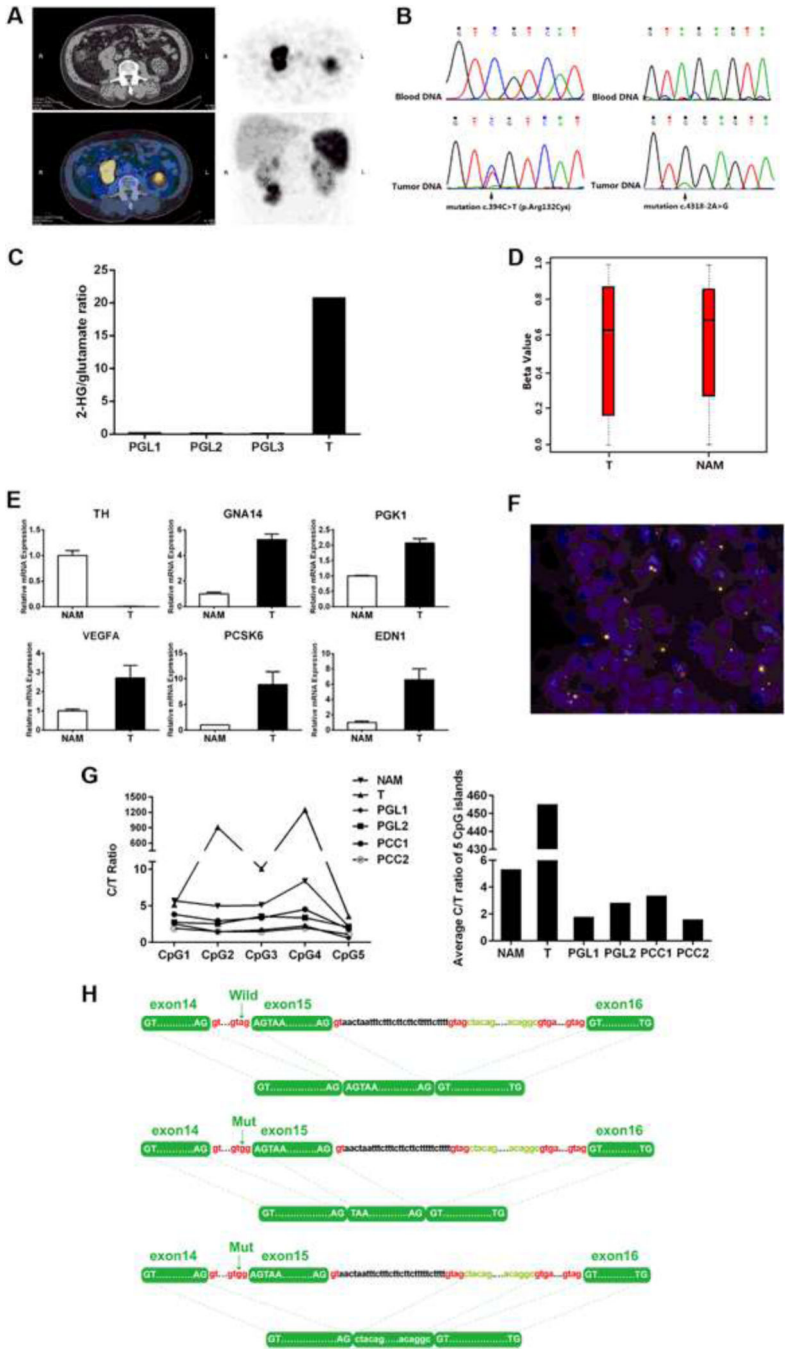

Fig. 1.

a A paraganglioma below the right kidney detected by computed tomography and Octreoscan. **b** Heterozygous mutation c.394C > T in exon 4 of the *IDH1* gene and heterozygous mutation c.4318–2A > G at the 5’ end of exon 15 of the *ATRX* gene were identified in the tumor DNA, but not in the peripheral blood DNA. **c** 2-Hydroxyglutarate (2-HG) /glutamate ratios assessed by GC-MS in the *IDH1*-mutant paraganglioma (T), compared with three paragangliomas (PGLs) without *IDH1* mutation. **d** Global methylation levels calculated by the beta value of the paraganglioma (T) and a normal adrenal medulla

(NAM). The beta values were reported as mean and standard deviation. **e** Quantitative mRNA expression measurement of *TH* gene and five hypoxia-related genes, namely *GNA14*, *PGK1*, *GLUT1*, *VEGFA*, *PCK6*, and *EDN1*. The *TH* gene encoding the rate-limiting enzyme in the synthesis of catecholamines performed by quantitative PCR assay. A normal adrenal medulla (NAM) specimen was used as a control. The bars indicate standard deviation. **f** Telomere-specific fluorescent *in situ* hybridization showed alternative lengthening of telomeres in the tumor cells (×1000). **g** Methylation levels of 5 CpG islands at the first exon of the *TH* gene from the current paraganglioma(T), normal adrenal medulla(NAM), two catecholamine-secreting paragangliomas (PGLs), and two catecholamine-secreting pheochromocytomas (PCCs). **h** Schematic illustration of alternative splicing caused by the *ATRX* mutation. The somatic-splicing mutation (c.4318–2A > G) of *ATRX* gene resulted in two alternative transcripts, one transcript skipped the first 2 base pairs of the exon 15, while the other one skipped the entire exon 15

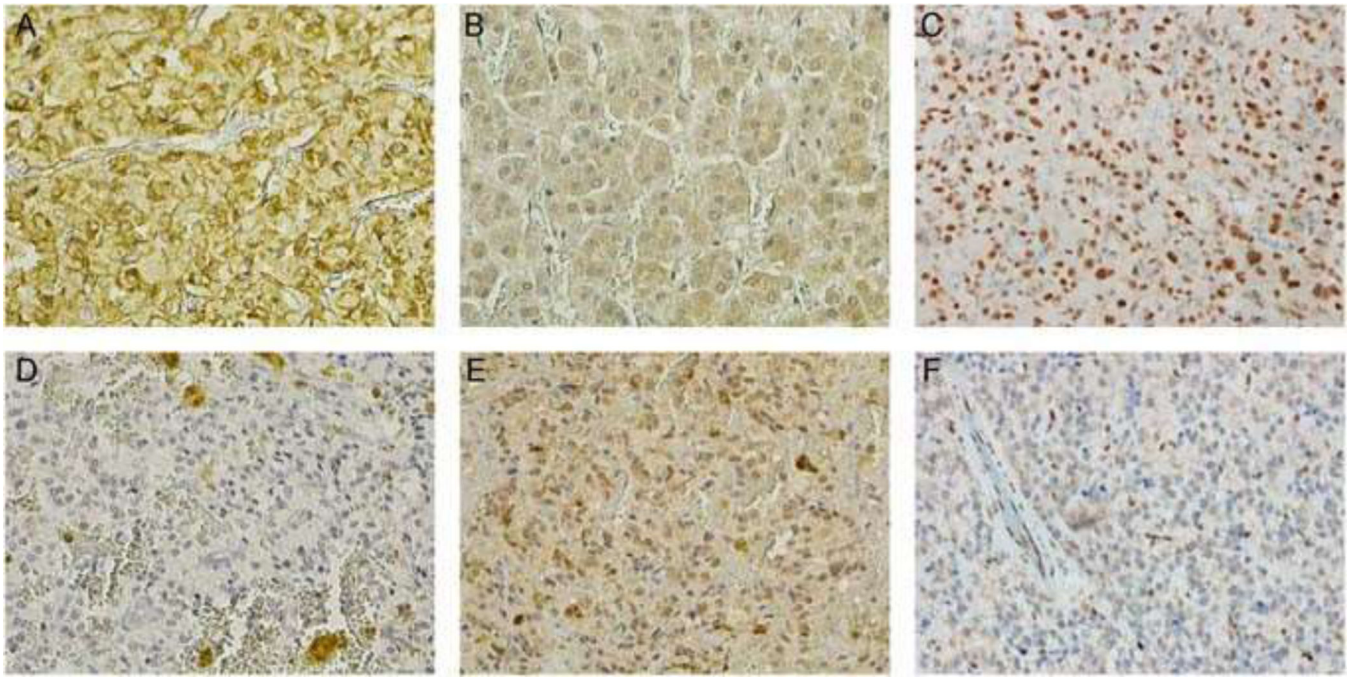

Fig. 2.

Tyrosine hydroxylase staining was scarce in the current paraganglioma (×400) **d**, with staining in a normal adrenal medulla as positive control (×400) **a**. HIF1α staining was strongly positive in the current paraganglioma (×400), **e** compared with that of a normal adrenal medulla (×400) **b**. Nuclear ATRX staining was scarce in the current paraganglioma (×400) **f**, with ATRX staining in a paraganglioma without ATRX mutation as a positive control (×400) **c**